Journal of Biosensors & Bioelectronics

Chen et al., J Biosens Bioelectron 2015, 6:2
DOI: 10.4172/2155-6210.1000173

Research Article Open Access

EDC-Mediated Oligonucleotide Immobilization on a Long Period Grating Optical Biosensor

Xianfeng Chen[1]*, Chen Liu[1], Marcus D Hughes[2], David A Nagel[2], Anna V Hine[2] and Lin Zhang[3]

[1]School of Electronic Engineering, Bangor University, Bangor LL57 1UT, UK
[2]School of Life and Health Sciences, Aston University, Birmingham B4 7ET, UK
[3]Aston Institute of Photonic Technologies, Aston University, Birmingham B4 7ET, UK

Abstract

We present the development and simplification of label-free fiber optic biosensors based on immobilization of oligonucleotides on dual-peak long period gratings (dLPGs). This improvement is the result of a simplification of biofunctionalization methodology. A one-step 1-ethyl-3-(3-dimethylaminopropyl) carbodiimide (EDC)-mediated reaction has been developed for the straightforward immobilization of unmodified oligonucleotides on the glass fiber surface along the grating region, leading to covalent attachment of a 5´-phosphorylated probe oligonucleotide to the amino-derivatized fiber grating surface. Immobilization is achieved via a 5´phosphate-specific linkage, leaving the remainder of the oligonucleotide accessible for binding reactions. The dLPG has been tested in different external media to demonstrate its inherent ultrahigh sensitivity to the surrounding-medium refractive index (RI) achieving 50-fold improvement in RI sensitivity over the previously-published LPG sensor in media with RI's relevant to biological assays. After functionalization, the dLPG biosensor was used to monitor the hybridization of complementary oligonucleotides showing a detectable oligonucleotide concentration of 4 nM. The proposed one-step EDC reaction approach can be further extended to develop fiber optic biosensors for disease analysis and medical diagnosis with the advances of label-free, real-time, multiplex, high sensitivity and specificity.

Keywords: Optical fiber biosensor; Long period grating; Label-free; Oligonucleotide; DNA; EDC-mediated reaction

Introduction

Biosensors have been developed to play a significant analytical role in medicine, diagnosis, life science, food, security and defense, environmental and industrial monitoring [1]. The traditional methods based on culture collection and colony counting were complicated, hazardous, expensive, time consuming and may require signal amplification or labeling. To overcome these drawbacks, the development of a portable, easy-to-use and highly sensitive biosensor for label-free and real-time detection is essential [2].

Over the past decade, the fiber optic biosensor has attracted great attention and made rapid advances [3,4]. Besides the inherent advantages exhibited by fiber technology, such as compact size, light weight, and electromagnetic interference immunity, fiber sensing platforms can provide higher sensitivity and selectivity than the traditional sensors. Recently, an emerging novel platform, the 'lab-on-fiber' was proposed for biotechnology and molecular biology applications [5,6]. The most important advantages of this biosensor platform are that it is able to provide biosensing with unique features of label-free, real-time, multiplex, and in-line determination. Various fiber optic biosensors have been presented by employing long period gratings (LPGs) [7,8], tilted fiber gratings (TFGs) [9-11] micro fiber Bragg gratings (mFBGs) [12] LPGs in photonic crystal fibers [13] and surface plasmon resonance (SPR) [14].

A long period grating is formed typically by photo inducing a periodic refractive index (RI) modulation in the order of hundreds of micrometers in the fiber core, which promotes the light coupling from the fundamental core mode to a set of forward-propagating cladding modes. The mode coupling verifying the phase-matching condition results in the transmission spectrum consisting of a series of attenuation peaks appearing at discrete wavelengths [15,16]. The LPG attenuation peaks correspond to the cladding guided modes with increasing evanescent fields extending outside the cladding boundary. External perturbation affects the evanescent field surrounding the LPG and so changes the cladding effective indices, thereby inducing the measurable wavelength shift of LPG resonances [17]. The evanescent field decays away from the surface of an optical fiber in a distance of a few micrometers [14], which is sufficient to penetrate into surrounding medium and sense its optical properties. Hence, LPGs can be used to detect changes when a target bioanalyte interacts with a recognition element on the LPG sensor [8,18].

It has been reported that the maximum refractive index sensitivity of the LPG can be achieved when the surrounding refractive index approaches the value of the fiber cladding [17]. This is far from the RI range 1.33-1.35 RIU (refractive index unit) of aqueous solutions where bioassays and biochemical events are typically carried out. Thus, in order to improve the RI sensitivity of the LPGs, several approaches have been investigated, such as etching the cladding, polishing the side and tapering the fiber [18-20]. However, those approaches become more complex and increase cost in terms of requiring careful packaging to compensate for the inevitable reduction in the mechanical integrity of the fiber [21]. An alternative approach for the enhancement of RI sensitivity has also been proposed by depositing a thin film overlayer of a material with RI higher than that of cladding [22], but this method lengthens sensor fabrication processes and requires additional time-consuming chemical treatments onto the fiber. In contrast, a unique property of the dual-peak LPG (dLPG) has been revealed whereby a

***Corresponding author:** Xianfeng Chen, School of Electronic Engineering, Bangor University, Bangor LL57 1UT, UK, Tel: +44 1248 382480; Fax: +44 1248 361429; E-mail: x.chen@bangor.ac.uk

Received May 28, 2015; **Accepted** June 08, 2015; **Published** June 28, 2015

Citation: Chen X, Liu C, Hughes MD, Nagel DA, Hine AV, et al. (2015) EDC-Mediated Oligonucleotide Immobilization on a Long Period Grating Optical Biosensor. J Biosens Bioelectron 6: 173. doi:10.4172/2155-6210.1000173

set of dispersion-turning-points exists in LPG phase-matching curves, resulting in the conjugate cladding modes observed as dual-peak features in the transmission spectrum [7,23,24]. Since they are in close proximity to the dispersion- turning-point, the dual-peak cladding modes are extremely sensitive to the surrounding-medium refractive index (SRI) change. As described above, the evanescent field extends a few microns beyond the fibre [14], but for dLPG-based RI sensors, the perturbation caused by surrounding RI change increases the effective refractive index of the fiber cladding modes, thereby causing measurable wavelength shifts of LPG's resonances. Unsurprisingly therefore, these simply fabricated dLPGs have recently been developed as biosensors [25].

Biosensing platforms are based on immobilized biomolecules for the detection of target analytes. The sensing biomolecules should be firstly bound to the sensor surface, then the biological recognition event generates a quantifiable signal corresponding to the concentration or RI change of the analytes. Thus, surface immobilization of biological probes (DNA, aptamers, antibodies, enzymes, etc.) plays a crucial role in the development of the biosensor. To date, various fiber optic biosensors have been developed for the detection of antibody-antigen interactions [26] DNA hybridization [8,27], biotin-streptavidin [28], cellular behavior [14], enzyme-glucose binding [11,29], and specific detection of bacteria using bacteriophages [25]. DNA biosensor technology is becoming an important area of high throughput research in basic biological and disease pathways. Different immobilization strategies have been proposed to bind oligonucleotides on a glass surface. Covalent linkage becomes the preferred approach as it allows a more stable attachment for hybridization. 1-ethyl-3-(3-dimethylaminopropyl) carbodiimide (EDC)-based coupling is used routinely in protein immobilization (via amino/carboxy-mediated coupling) and has also been applied to covalently attach DNA molecules to a diamond surface via the 5′-phosphate group [30].

Here we present, for the first time, a one-step EDC-mediated reaction for the immobilization of oligonucleotides on dLPG-based biosensors. EDC and imidazole reagents lead to the formation of a phosphoramidate linkage between amino-derivatized glass fiber surface and 5′-phosphate modified oligonucleotides in a one-step reaction. The improvement and simplification of biomolecule immobilization procedure is feasible by using only EDC as the heterobifunctional cross-linker for 5′-phosphorylated oligonucleotides. The functionalized dLPG has also been used for experimentally monitoring the hybridization of complementary oligonucleotides in real-time, showing a high sensitivity, specificity and lower limit of detection.

Materials and Methods

Materials

(3-Aminopropyl) triethoxysilane (APTES), 1-ethyl-3-(3-dimethylaminopropyl) carbodiimide (EDC), 1-methylimidazole, phosphate buffered saline (PBS), and SSPE buffer were purchased from Sigma-Aldrich (United Kingdom). Hydrochloric acid (HCl), deionized (DI) water, and methanol were purchased from Thermo Fisher Scientific Inc. (United Kingdom). The Cargille refractive index matching liquids (Range 1.300 to 1.458, Adjusted to ± 0.0002) were purchased from Cargille Laboratories, Inc. (United States).

Nucleic acid preparation: The 5'-ends of oligonucleotides were modified during synthesis with the phosphate group. Oligonucleotides (Carl Roth, Karlsruhe) were designed as follows:

Probe: 5'-phosphate-GCA CAG TCA GTC GCC-3'

Complementary: 5'-GGC GAC TGA CTG TGC-3'

Fabrication of dual-peak long period gratings

To obtain the dual-peak feature, the periods ranging from 140 μm to 160 μm were selected and designed for the fabrication of dLPGs. 3 cm long dLPGs were UV inscribed in hydrogenated standard single-mode fiber (SMF28, Corning) by a CW frequency-doubled Ar laser (244 nm) using the point-by-point fabrication method over multiple iterations. After UV inscription, the gratings were annealed at 80°C for 48 h to remove the residual hydrogen and to stabilize their optical properties.

Surface functionalization of fiber sensor

To generate a fiber optic biosensor, it is necessary to immobilize one of the two interacting biomolecules on the sensor surface. Figure 1 depicts an overview of fiber optic biosensor generation, including each step of the functionalization from the bare glass fiber surface to probe oligonucleotide immobilization and to the final hybridization with the complementary DNA sequence. Individual stages are detailed below.

Glass fiber surface pre-treatment and silanization: The successful amino functionalization of LPG's with (3-aminopropyl)triethoxysilane (APTES) has been well- documented for use in protein immobilization [8, 11,29], as determined by fluorescent microscopy of the subsequently-immobilized protein [8,11]. We therefore employed this method of

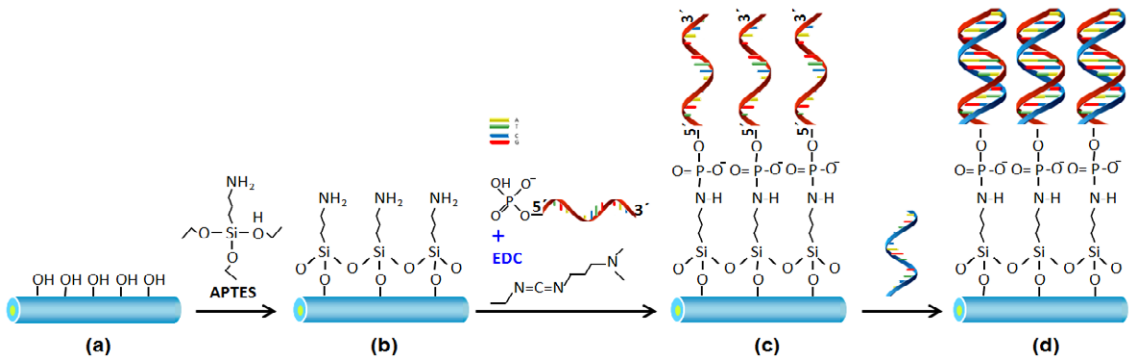

Figure 1: Schematic diagram of biofunctionalization of fiber optic biosensor: (a) Cleaned glass fiber surface. (b) Silanization of glass fiber surface by APTES. (c) Covalent immobilization of 5′-phosphorylated oligonucleotides via EDC-mediated reaction. (d) Hybridization with the complementary oligonucleotides.

amino functionalization in the current study. Briefly, the glass fiber (in the region of the grating) was soaked in freshly-prepared 5 M HCl solution for 30 min, thoroughly rinsed with deionized (DI) water then dried in the air (Figure 1a). It was then immersed in a fresh, 10% solution of APTES for 50 min this reaction generated surface primary amine groups (Figure 1b), ready for EDC coupling. The fiber sensor was then rinsed with DI water and again air-dried.

EDC-mediated oligonucleotide immobilization: In this process, EDC and imidazole reagents lead to the formation of a phosphoramidate linkage between the amino-silanized fiber glass surface and the 5´-phosphate group on the oligonucleotide, in a one-step reaction.

An aqueous solution of 5'-phosphorylated oligonucleotide (5'-phosphate-GCA CAG TCA GTC GCC-3') was diluted with 30 mM 1-methylimidazole to a final concentration of 5 μM and 10 mg/ml EDC was added and mixed for 1 min. The amino-silanized glass fiber was immediately immersed into this oligonucleotide solution, which was placed in a closed container to avoid evaporation, and incubated overnight at room temperature. After 16.5 h incubation, the glass fiber was thoroughly rinsed in DI water, dried in the air and stored in dry container at room temperature for further use (Figure 1c). The oligonucleotide was now covalently-linked to the biosensor and available for hybridization to a complementary DNA strand (Figure 1d).

Device and data analysis

All the biochemical experiments were performed in a fume cupboard (Labcaire Systems Ltd, UK). To minimize the bend cross-sensitivity, the fiber grating sensors were placed straight in a custom-made V-groove container on a Teflon plate and all the chemicals and solvents were added and withdrawn from the container by careful pipetting.

In the interrogation system, broadband light sources (BBS: Agilent HP83437A, Agilent Technologies Inc.; LS-1 Tungsten Halogen Light Source, Ocean Optics Inc.) were used along with an optical spectrum analyzer (OSA, Agilent HP86142A, Agilent Technologies Inc., range 600 nm to 1700 nm). The OSA was connected to a computer and the optical spectra were captured by a customized program. Data analysis was performed using that customized program which automatically defines resonance wavelengths, using the centroid calculation method.

Results and Discussion

Dual-peak features during dLPG fabrication

An LPG in a single mode fiber couples the light from the core mode to co-propagating cladding modes resulting in the transmission spectrum containing a series of attenuation bands. Each attenuation band corresponds to the coupling to a cladding mode satisfying the phase-matching condition [15].

$$\lambda_{res} = (n_{co}^{eff} - n_{cl,m}^{eff})\Lambda$$

where Λ is the grating period, n_{co}^{eff} and $n_{cl,m}^{eff}$ are the effective indices of core and mth cladding mode. It has been reported that a set of dispersion turning points exists on the phase-matching curves due to the parabolic property of the group index of the higher cladding modes [7]. With a selected relatively short LPG period, the light coupling between the fundamental core mode and a higher order cladding mode leads to two attenuation peaks in the transmission spectrum with respect to the conjugate cladding mode. LPGs with such dual-peak features are defined as dual-peak LPGs (dLPGs).

The graphic phase curves for a 157 μm-period dLPG are plotted in Figure 2a, where the dots marked on the top of the curves represent the dispersion-turning-points. The intersection points of phase curves and the horizontal line are the wavelengths at which the phase-matching conditions are satisfied. For the 12th cladding mode, there are two resonances sitting on both sides of the turning point, LP_{012}^{blue} and LP_{012}^{red} which are defined as 'blue-peak' (short wavelength) and 'red-peak' (long wavelength), respectively.

Point-by-point and multiple scanning methods were employed to inscribe the dLPG (3 cm long, 157 μm period). During the UV inscription process, the dLPG spectra were recorded. Development of the dual-peak characteristics can be clearly observed during the multiple scans (Figure 2b). After the first cycle of UV exposure, there was no noticeable peak (Figure 2b, black). In the second cycle, two resonances initially appeared at 1180 nm (LP_{012}^{blue}) and 1630 nm (LP_{012}^{red}), (Figure 2b, green) which moved towards each other with subsequent inscriptions (Figure 2b, orange and purple). During the third cycle (Figure 2b, orange), dual peaks were moving closer and growing stronger while a new resonance corresponding to the LP011 cladding mode was generated at 1010 nm. With further UV exposure in fourth cycle (Figure 2b, purple), the dual peaks moved more closer and became stronger, whereas the LP011 peak showed only a small red-shift. The spectral evolution can be explained by Figure 2a. Successive UV exposures increased the core effective refractive index, causing the phase curve to move downwards (Figure 2a, green→orange→purple). Thus the two intersection points (LP_{012}^{blue} and LP_{012}^{red}) corresponding to the same LP012 cladding mode made a large movement wherein the separation between these intersections reduced from 450 nm to 150 nm (Figure 2a, red and blue dotted arrows). This movement, as dual peaks close towards the dispersion-turning-point, forms the basis for an extremely sensitive detector. Thus, as the UV inscription progressed, the blue-peak was red-shifted whereas the red-peak made the opposite blue-shift. In contrast, the movement of the phase curve with successive UV inscriptions has relatively little effect on the LP011 peak, causing only a slight red-shift and a weak increase in strength.

Refractive index sensitivity characteristics of dLPG

The RI sensitivity was investigated by immersing the dLPG in a set of index gels (Cargille Lab Inc. US). The spectrum was measured for each RI value, the wavelength shift of dLPG resonances are plotted in Figure 2c and the spectral features are depicted in Figure 2d. Over the range of RIs from 1.30 to 1.44, the red-peak LP_{012}^{red} is further red-shifted with increasing RI, whereas the blue-peak LP_{012}^{blue} is further blue-shifted. In contrast, the LP011 peak shows only a slight blue-shift with increasing RI. It can be seen from Figure 2c that the resonances move nonlinearly with an increasing trend over the whole RI range. The total wavelength shifts of LP011, LP_{012}^{blue} and LP_{012}^{red} are -10.6 nm, -111.7 nm, and +225.0 nm respectively (with a calculated estimation for the final red-peak which had moved out of the detectable range). The detail of RI characteristics for different peaks are compared and listed in Table 1. It is particularly noteworthy that both the blue and red peaks show an ultrahigh RI sensitivity of -2914 nm/RIU and +7488 nm/RIU in the high RI range (1.432 to 1.44; Table 1), respectively, whereas

Resonance	LP_{011}	LP_{012}^{blue}	LP_{012}^{red}
High RI (n: 1.432-1.44)	-288	-2914	7488
Low RI (n: 1.30-1.35)	-26	-564	794

Table 1: RI sensitivity (nm/RIU) characteristics of dual-peak LPG.

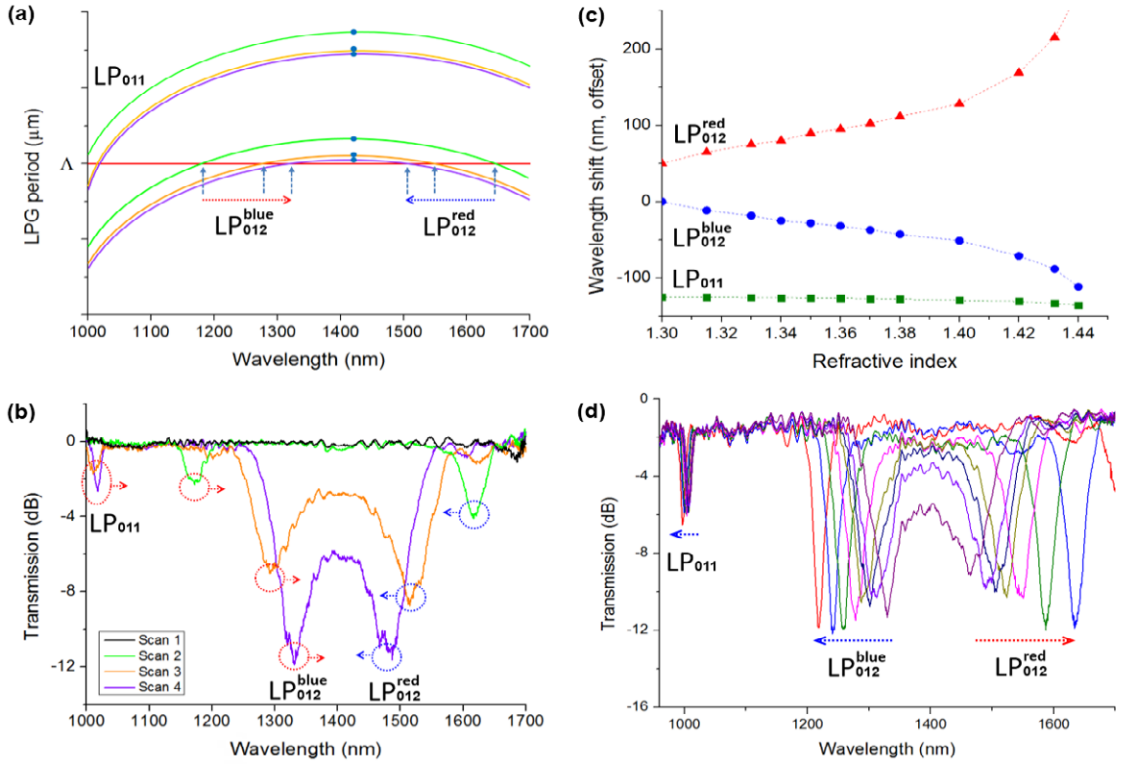

Figure 2: Dual-peak LPG fabrication process: (a) Phase-matching curves for analysis of movement of dual peaks. (b) Spectral evolution under UV exposure. Dual-peak LPG RI sensitivity experiment: (c) Wavelength shift of dLPG resonances. (d) Transmission spectrum change against SRI.

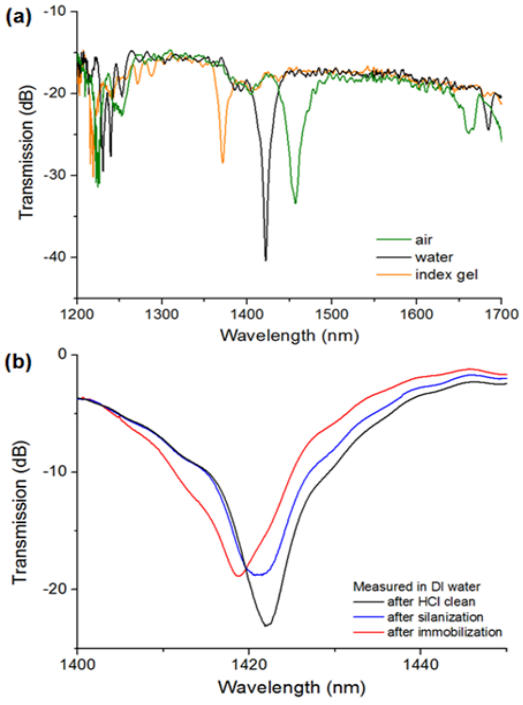

Figure 3: (a) dLPG spectrum measured in different surrounding media. (b) Spectra captured in DI water after cleaning, silanization and oligonucleotide immobilization.

the LP011 peak has a low sensitivity of -288 nm/RIU. The blue and red peaks also show high RI sensitivity of -564 nm/RIU and +794 nm/RIU, respectively, in low RI range (1.30 to 1.35; Table 1) – the range in which bioassays and biochemical event-monitoring are usually carried out. The maximum RI sensitivity (794 nm/RIU) in low range RIs of 1.30-1.35 of our dLPG is more than 50 times higher than that of previously reported 370 μm period LPG sensor, who achieved an RI sensitivity of 15 nm/RIU around 1.33 RIU [31]. Hence, biosensors based on dLPGs should achieve comparable or better performances with respect to the standard LPG or mFBG based biosensors [12,31].

Evaluation of oligonucleotide attachment

The biofunctionalization of the dLPG sensor was determined by monitoring the spectral evolution of dLPG in situ throughout the cleaning, silanisation and immobilization processes.

A 3 cm-long dLPG with a period of 158.5 μm was used for this experiment. As shown in Figure 3a, there are three resonances within the observed wavelength range. Consistent with previous observations (Figure 2d), when transmission spectra were measured in different RI media, separation between peaks in the 1300-1700 nm increases with increasing RI, which confirms that they are dual peaks corresponding to the same conjugate cladding mode. In our work, the blue-peak at 1422 nm (in water) was selected for the following experiments.

Figure 3b shows the transmission spectra of this peak, captured in DI water, after HCl cleaning, APTES silanization, and oligonucleotide immobilization, respectively. A clear blue-shift has occurred in response to this biofunctionalization procedure. Specifically, the silanization

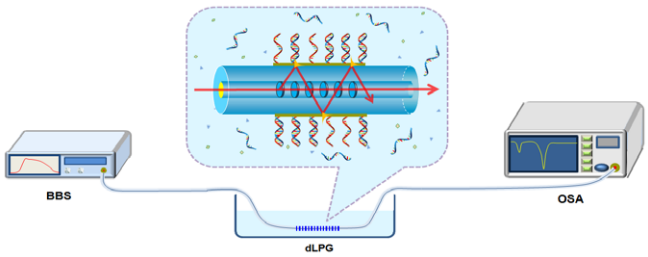

Figure 4: Experimental setup for fiber grating based biosensor sensing system. Inset: schematic diagram of hybridization process between probe oligonucleotide immobilized dLPG biosensor and complementary oligonucleotides.

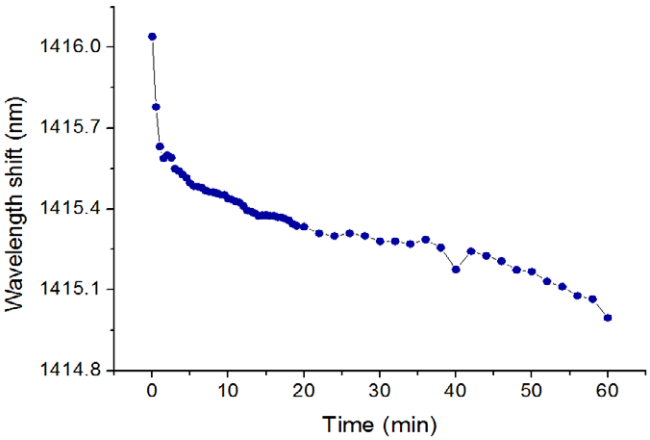

Figure 5: Wavelength shift against time during the DNA hybridization process.

has induced a relatively small blue-shift of -1024 pm whereas the immobilization has moved the peak by a further -2320 pm. Clearly, the APTES- modification and the attachment of 5′-phosphorylated oligonucleotides on the fiber grating surface have each changed the effective index of cladding, so demonstrating successful immobilization.

Hybridization of complementary oligonucleotides

The dLPG sensor with immobilized oligonucleotide was next hybridized with a complementary oligonucleotide (5'-phosphate-GCA CAG TCA GTC GCC-3'). The optical spectral evolution during the hybridization process was monitored by the use of the optical interrogation system shown in Figure 4. The broadband source launches the light into the dLPG biosensor whose spectrum is monitored by OSA.

Following DNA immobilization (Figure 1c), the dLPG sensor was washed in DI water and rinsed in 6 × SSPE buffer (0.9 M NaCl, 0.06 M NaH_2PO_4, and 0.006 M EDTA) for 10 min, then immersed in fresh 2 μM complementary oligonucleotide in 6 × SSPE buffer and allowed to react at room temperature for 60 min.

The blue-peak LP_{012}^{blue} described above was monitored in situ throughout the whole hybridization process. As can be seen from Figure 5, the resonant peak shows a blue-shift of -1044 pm over the whole hybridization process. There are three stages associated with the 60 min DNA hybridization. A rapid reaction occurs in the first 3 min with the wavelength shift of -490 pm, which equates to a detection sensitivity of 245 pm blue-shift per μM DNA (or 4 nM DNA per pm blue-shift). This initial reaction is followed by a steady process (3 to 20 min) with the wavelength shift of -216 pm, and finally a much slower reaction (20 to 60 min) with the shift of -338 pm. Thus maximum sensitivity occurs in the first 3 mins.

Although not described herein, it is therefore feasible that the dLPG sensor could be used to study binding kinetics. The sensor measurements are rapid (503 ms per full scan for the selected 'blue-peak') and in the current study, measurements were taken every 30s for the first 20 mins. However, the measurement time could easily be reduced to 1 scan/s and the resulting data used to give kinetic analyses of initial rates of binding. Finally, if the noise effect could be eliminated effectively by using an optical interrogation system with 1 pm resolution, this would theoretically lead to a detection sensitivity of 4 nM oligonucleotide concentration, which would be two orders of magnitude lower than the microfiber Bragg grating based DNA biosensor reported previously [12].

Conclusion

We have successfully demonstrated a label-free biosensor based on a dual-peak LPG to detect the hybridization of oligonucleotides in real-time. The dual-peak LPG with inherent ultrahigh/high RI sensitivity has been demonstrated to detect a quantifiable optical signal corresponding to the refractive index change of the bio-analytes in which the biological recognition events occurred. Moreover, a one-step EDC-mediated procedure has been demonstrated to facilitate the covalent immobilization of 5′-phosphorylated oligonucleotide on an amino-modified glass fiber sensor surface. Although only DNA hybridization of a complementary oligonucleotide has been demonstrated herein, the technology also has similar potential for use in future aptamer-based binding studies.

Acknowledgement

The authors are grateful for the support from the projects of FP7 PIRSES-2013-612267 and the Ser Cymru NRN.

References

1. Marks RS, Lowe CR, Cullen DC, Weetall HH, Karube I (2007) Handbook of Biosensors and Biochips. Wiley, Weinheim. Overview of biosensor and bioarray technologies.
2. Estevez M, Otte MA, Sepulveda B, Lechuga LM (2014) Trends and challenges of refractometric nanoplasmonic biosensors. Analytica Chimica Acta 806: 55-73.
3. Fan X, White IM (2011) Optofluidic microsystems for chemical and biological analysis. Nature Photonics 5: 591-597.
4. Wang XD, Wolfbeis OS (2008-2012) (2013) Fiber-optic chemical sensors and biosensors. Anal Chem. 85: 487-508.
5. Canning J (2009) Properties of specialist fibres and Bragg gratings for optical fibre sensors. J of Sensors 2009: 1-17.
6. Cusano A, Consales M, Crescitelli A, Ricciardi A (eds.) (2014) Lab-on-Fiber Technology. Springer.
7. Shu X, Zhang L, Bennion I (2002) Sensitivity characteristics of long-period fiber gratings. J Lightwave Technol 20: 255-266.
8. Chen X, Zhang L, Zhou K, Davies E, Sugden K, et al. (2007) Real-time detection of DNA interactions with long-period fiber-grating-based biosensor. Opt Lett 32: 2541-2543.
9. Albert J, Shao LY, Caucheteur C (2013) Tilted fiber Bragg grating sensors. Laser Photonics 7: 83-108.
10. Caucheteur C, Shevchenko Y, Shao L, Wuilpart M, Albert J (2011) High resolution interrogation of tilted fiber grating SPR sensors from polarization properties measurement. Opt Express 19: 1656-1664.
11. Luo B, Yan Z, Sun Z, Li J, Zhang L (2014) Novel glucose sensor based on enzyme-immobilized 81° tilted fiber grating. Opt Express 22: 30571-30578.

12. Sun D, Guo T, Ran Y, Huang Y, Guan BO (2014) In-situ DNA hybridization detection with a reflective microfiber grating biosensor. Biosens Bioelectron 61: 541-546.

13. He Z, Tian F, Zhu Y, Lavlinskaia N, Du H (2011) Long-period gratings in photonic crystal fiber as an optofluidic label-free biosensor. Biosens Bioelectron 26: 4774-4778.

14. Shevchenko Y, CamciUnal G, Cuttica D, Dokmeci M, Albert J, et al. (2014) Surface plasmon resonance fiber sensor for real-time and label-free monitoring of cellular behavior. Biosens Bioelectron 56: 359-367.

15. Vengsarkar A, Lemaire P, Judkins J, Bhatia V, Erdogan T, et al. (1996) Long-period fiber gratings as band-rejection filters. J Lightwave Technol 14: 58-64.

16. Erdogan T (1997) Cladding mode resonances in short and long period fiber grating filters. J Opt Soc Am 14: 1760-1773.

17. Patrick HJ, Kersey A, Bucholtz F (1998) Analysis of the response of long period fiber gratings to external index of refraction. J Lightwave Technol 16: 1606-1611.

18. Jang HS, Park KN, Kim JP, Sim SJ, Kwon OJ, et al. (2009) Sensitive DNA biosensor based on a long-period grating formed on the side-polished fiber surface. Opt Express. 17: 3855-3860.

19. Chen X, Zhou K, Zhang L, Bennion I (2005) Simultaneous measurement of temperature and external refractive index by use of a hybrid grating in D fiber with enhanced sensitivity by HF etching. Appl Opt 44: 178-182.

20. Ding J, Zhang A, Shao LY, Yan JH, He S (2005) Fiber-taper seeded long-period grating pair as a highly sensitive refractive-index sensor. IEEE PhotonTechnol Lett 17: 1247-1249.

21. James SW, Tatam RP (2003) Optical fibre long-period grating sensors characteristics and application. Meas Sci Technol 14: 49-61.

22. Pilla P, Trono C, Baldini F, Chiavaioli F, Giordano M, Cusano A (2012) Giant sensitivity of long period gratings in transition mode near the dispersion turning point: an integrated design approach. Opt Lett 37: 4152-4154.

23. Chen X, Zhou K, Zhang L, Bennion I (2007) Dual-peak long-period fibre gratings with enhanced refractive index sensitivity by finely tailored mode dispersion that uses the light cladding etching technique. Appl Opt 46: 451-455.

24. Smietana M, Koba M, Mikulic P, Bock WJ, (2014) Measurements of reactive ion etching process effect using long-period fiber gratings. Opt Express 22: 5986-5994.

25. Brzozowska E, Smietana M, Koba M, Gorska S, Pawlik K, et al. (2015) Recognition of bacterial lipopolysaccharide using bacteriophage-adhesin-coated long-period gratings. Biosens. Bioelectron 67: 93-99.

26. Chiavaioli F, Biswas P, Trono C, Bandyopadhyay S, Giannetti A, et al. (2014) Towards sensitive label-free immunosensing by means of turn-around point long period fiber gratings. Biosens Bioelectron 60: 305-310.

27. Yin M, Wu C, Shao LY, Chan W, Zhang P, et al. (2013) Label-free, disposable fiber-optic biosensors for DNA hybridization detection. Analyst 138: 1988-1994.

28. Voisin V, Pilate J, Damman, P, Mégret P, Caucheteur C (2014) Highly sensitive detection of molecular interactions with plasmonic optical fiber grating sensors, Biosensors and Bioelectronics. Biosens Bioelectron 51: 249-254.

29. Deep A, Tiwari U, Kumar P, Mishra V, Jain S, et al. (2012) Immobilization of enzyme on long period grating fibers for sensitie glucose detection. Biosens Bioelectron 33: 190-195.

30. Christiaens P, Vermeeren V, Wenmackers S, Daenen M, Haenen K, et al. (2006) EDC-mediated DNA attachment to nanocrystalline CVD diamond films. Biosens Bioelectron 22: 170-177.

31. Chiavaioli F, Trono C, Giannetti A, Brenci M, Baldini F (2014) Characterisation of label-free biosensor based on long period grating. J. Biophotonics 7: 312-322.